

SPECTRAL METHODS FOR NEURAL INTEGRAL EQUATIONS

EMANUELE ZAPPALA

ABSTRACT. Neural integral equations are deep learning models based on the theory of integral equations, where the model consists of an integral operator and the corresponding equation (of the second kind) which is learned through an optimization procedure. This approach allows to leverage the nonlocal properties of integral operators in machine learning, but it is computationally expensive. In this article, we introduce a framework for neural integral equations based on spectral methods that allows us to learn an operator in the spectral domain, resulting in a cheaper computational cost, as well as in high interpolation accuracy. We study the properties of our methods and show various theoretical guarantees regarding the approximation capabilities of the model, and convergence to solutions of the numerical methods. We provide numerical experiments to demonstrate the practical effectiveness of the resulting model.

CONTENTS

1. Introduction	1
2. Methods	2
3. Theoretical framework and approximation capabilities	4
4. Algorithm	10
5. Experiments	10
5.1. Integral Equations Dataset	11
5.2. Simulated fMRI Dataset	12
References	13

1. INTRODUCTION

The theory of integral equations (IEs) has found important applications in several disciplines of science. In physics, for example, integral operators and integral equations are found in the theory of nonlocal gravity [10], plasma physics [27], fluid dynamics [3], and nuclear reactor physics [1]. Several applications are also found in engineering [26], brain dynamics [2, 28], and epidemiology [12]. Such a wide range of applications has therefore motivated the study of IE and integro-differential equation (IDE) models in machine learning, for operator learning tasks [30, 31]. These models are called neural IEs (NIEs) and neural IDEs (NIDEs), respectively. They need to solve an IE or IDE at each step of the training (and for each data sample), therefore incurring in significant computational costs. While there is a benefit in modeling dynamics using neural IEs and IDEs due to the nonlocality of the integral operators, it is of interest to obtain formulation of these models that are more computationally efficient.

Operator learning is a branch of machine learning where the training procedure aims at obtaining an operator acting in an infinite dimensional space of functions. The theoretical foundation of operator learning has been significantly developed in [24], based on results dating back to the 90's,

and more recently found examples in several other works, e.g. [15, 16, 18, 22]. Operator learning allows to learn the governing equations of a system from data alone, without further assumptions or knowledge on the properties of the system that generated the dataset. As such, it is greatly useful in studying complex systems whose theoretical properties are not completely understood.

The scope of this article is to introduce a framework for neural IEs, which is an operator learning problem, based on spectral methods. This allows to perform integration in the spectral domain, greatly simplifying the architecture of the models, but still retaining their great modeling capabilities of NIEs, especially in regards to long range dependencies (high nonlocality).

The convenience of this method with respect to the approach to neural network approaches for learning integral operators in IEs and IDEs found in [30, 31] lies in the following facts:

- A small (in terms of parameters) neural network G_θ can achieve comparable expressivity and task accuracy to larger models;
- Integration in this setting consists only of a matrix multiplication as opposed to quadrature rules or Monte Carlo methods, therefore improving computational speed and memory scalability of the model;
- The output of the spectral IE solver implemented in this article is a solution \mathbf{y} which is expanded in the Chebyshev basis, and that can therefore be easily interpolated.

Overall, this method produces highly smooth outputs that can be interpreted as denoised approximations of the dataset. Throughout this article we will use Chebyshev polynomials of the first kind, referring to them simply as Chebyshev polynomials without further specification.

The codes implemented for this method, and for the experiments found in Section 5, can be found at https://github.com/emazap7/Spectral_NIE.

2. METHODS

In this section we introduce and discuss the spectral approaches used in this article for integral operator learning. We consider the one dimensional case, where our method is based on Chebyshev polynomials, and defer a generalization of this methods to higher dimensions to a later work.

We consider integral equations of Fredholm and Volterra types which take the form

$$(1) \quad \mathbf{y}(t) = f(\mathbf{y}, t) + \lambda \int_{-1}^{\alpha(t)} G(\mathbf{y}, t, s) ds,$$

where $\alpha(t) = t$ for a Volterra equation, and $\alpha(t) = 1$ for a Fredholm equation, $G : \mathbb{R} \times [-1, 1] \times [-1, 1] \rightarrow \mathbb{R}$ is potentially non-linear function in \mathbf{y} called the *kernel*, and $\mathbf{y} : [-1, 1] \rightarrow \mathbb{R}$ is the unknown function. In this article we consider equations defined on the interval $[-1, 1]$, which are sufficient for the scope of machine learning in the assumption that the time intervals have been normalized. In the context of traditional IEs (with no learning), spectral approaches for linear equations in \mathbf{y} , where $G(\mathbf{y}, t, s) = K(t, s)\mathbf{y}$ have been treated in [23], while the nonlinear case where G has the form $G(\mathbf{y}, t, s) = K(t, s)\mathbf{y}^m$ for some $m > 1$ has been considered in [29]. In the present work, we consider arbitrary functions G where the learning process determines a neural network G_θ which is obtained through optimization on a given dataset. Our setup is an operator learning problem where we want to learn the integral operator by learning the parameters θ of G_θ , therefore obtaining

$$(2) \quad \mathbf{y}(t) = f(\mathbf{y}, t) + \lambda \int_{-1}^{\alpha(t)} G_\theta(\mathbf{y}, t, s) ds,$$

Let us denote by $C_j(t)$ the j^{th} Chebyshev polynomial and let N be a fixed natural number. We write the truncated Chebyshev series as

$$(3) \quad \mathbf{y}(t) \approx \mathbf{y}_N(t) := \sum_{j=0}^N a_j C_j(t),$$

where $a_j \in \mathbb{R}$ are coefficients that determine the expansion of \mathbf{y} in $C_j(t)$. The collocation points $\{t_k\}_{k=0}^N \subset [-1, 1]$ are optimally taken to be the Chebyshev collocation points $t_k = \cos(\frac{k\pi}{N})$ for $k = 0, \dots, N$, but we will experimentally show that the method is effective even when the points t_k are taken to be different from this choice, which is of importance since datasets might have arbitrary time stamps (including irregularly sampled time points).

Using Equation (3), from Equation (1) we obtain

$$(4) \quad \mathbf{y}(t_i) = f(\mathbf{y}(t_i), t_i) + \lambda \int_{-1}^{\alpha(t_i)} G\left(\sum_{j=0}^N a_j C_j(s), t_i, s\right) ds,$$

which we want to solve for all $i = 0, \dots, N$. Applying this setup to the case of integral operators parameterized by neural networks, we find the equation corresponding to Equation (4)

$$(5) \quad \mathbf{y}(t_i) = f(\mathbf{y}(t_i), t_i) + \lambda \int_{-1}^{\alpha(t_i)} G_\theta\left(\sum_{j=0}^N a_j C_j(s), t_i, s\right) ds.$$

In order to solve Equation (4) or Equation (5) we need an efficient way of computing the integrals $\int_{-1}^{\alpha(t_i)} G\left(\sum_{j=0}^N a_j C_j(s), t_i, s\right) ds$, and $\int_{-1}^{\alpha(t_i)} G_\theta\left(\sum_{j=0}^N a_j C_j(s), t_i, s\right) ds$ for all $i = 0, \dots, N$. Let us first consider the former case, where θ does not appear. For the moment we will only concern ourselves with being able to solve Equation (4), and Equation (5) for given parameters θ , without concerning ourselves with optimizing the parameters θ .

Observe that for each fixed spectral collocation point t_i , and fixed \mathbf{y} (hence fixed coefficients a_k), the function G induces a function $\hat{G}^i : [-1, 1] \rightarrow \mathbb{R}$ obtained through the correspondence $s \mapsto G\left(\sum_{j=0}^N a_j C_j(s), t_i, s\right)$. Here we suppress the dependence of \hat{G}^i on \mathbf{y} for notational simplicity. Similarly to how \mathbf{y} has been expanded through a truncated Chebyshev series we have

$$(6) \quad \hat{G}(s) \approx \hat{G}_N(s) := \sum_{r=0}^N b_r C_r(s),$$

for some coefficients b_r . In the assumption that the b_r are known, there is a computationally efficient method for computing the integral $\int_{-1}^{\alpha(t_i)} \hat{G}^i(s) ds$ through the coefficients of the Chebyshev expansion, given in [13, 14]. We recall these results for Fredholm and Volterra equations here.

First, let us denote by \mathfrak{X} the space of infinite sequences (a_0, \dots, a_n, \dots) of real numbers. We can express a function $\mathbf{y} : [-1, 1] \rightarrow \mathbb{R}$ as such a sequence by associating to \mathbf{y} its Chebyshev coefficients. In practice, we are interested in sequences that vanish after a certain $N \in \mathbb{N}$, since we consider in this article finite Chebyshev expansions. As such, we can express integral (Fredholm and Volterra) operators as mappings $\mathfrak{I} : \mathfrak{X} \rightarrow \mathfrak{X}$. Let $\mathbf{b} \in \mathfrak{X}$, and let $\hat{\mathbf{b}}$ denote the sequence obtained from \mathbf{b} by defining $\hat{b}_0 := 2b_0$, and setting $\hat{b}_n = b_n$ for all $n > 0$.

Then, (see [13, 14]) we define $\mathbf{d} := \mathfrak{I}(\mathbf{b})$ by the formula

$$(7) \quad d_k = \frac{\hat{b}_{k-1} - \hat{b}_{k+1}}{2k},$$

for all $k > 1$, and

$$(8) \quad d_0 = \sum_{i=1}^{\infty} (-1)^{i+1} d_i.$$

In this article, in practice, the latter is finite, as all the coefficients a_k are eventually zero (we only consider finite Chebyshev expansions), and we therefore will start using finite sums up to N , to explicitly take this fact into account. This mapping has been called spectral integration in [14], and we will follow this convention here. We can now define the Fredholm and Volterra integral operators in spectral form, \mathcal{J}_F and \mathcal{J}_V respectively, by the formulae

$$(9) \quad \int_{-1}^1 \hat{G}^i(s) ds = 2 \sum_{k=0}^N d_{2k+1}$$

$$(10) \quad \int_{-1}^{\alpha(t_i)} \hat{G}^i(s) ds = \frac{1}{2} d_0 + \sum_{k=1}^N d_k C_k(\alpha(t_i)),$$

for all spectral collocation points t_i , cf. Lemma 2.1 in [14] and the Appendix to [13].

Solving the IE problem in Equation (4) presents now the complication that once we have the Chebyshev expansion of \mathbf{y} , i.e. its coefficients a_n , $n \leq N$, we need to compute the Chebyshev coefficients b_n of G^i for each collocation point. This procedure requires an integration per collocation point in order to project the function G onto the Chebyshev basis. However, when our task is to learn the integral operator as in the present article, we can bypass the issue altogether, and learn the neural network G_θ as a mapping in spectral space, directly giving the correspondence $\mathbf{a} \mapsto \mathbf{b}$. Moreover, integration in this formulation simply accounts to performing a matrix multiplication, as seen in Equation (9) and Equation (10).

3. THEORETICAL FRAMEWORK AND APPROXIMATION CAPABILITIES

We can reformulate the method as described in Section 2 using a more general language. While this does not add any new information to the setup, it makes a general treatment simpler. In this regard, we let X denote a Banach space of functions of interest (whose precise definition depends on the problem considered), and we indicate the integral operator of Equation (1) by $T : X \rightarrow X$, where we assume that a choice of α is performed. In this article, the space X is assumed to be a Hölder space, for our theoretical guarantees. When the integral operator is parameterized by a neural network with parameters θ , we indicate it by T_θ when we want to explicitly make this fact clear.

We observe that the Chebyshev expansion considered in Equation (3) is the result of projecting a function $y \in X$ on the space X_N spanned by the first N Chebyshev polynomials. So, we have a projector (or projection operator) $P_N : X \rightarrow X_N$, the precise formulation of which will be given in the algorithm. Also, we notice that the spaces X_N of Chebyshev polynomials up to degree N are increasing $X_N \subset X_{N+1}$ and such that for each $y \in X$ the projections $P_N y := y_N$ satisfy $\|y - y_N\| \rightarrow 0$ as $N \rightarrow \infty$, under some regularity conditions that we will assume later in this section.

The method of Section 2 consists of approximating the integral equation $(\mathbb{1} - T)y = f$ through a function and a spectral integration on the Chebyshev space X_N , and solving the corresponding integral equation, which we denote by

$$(11) \quad (\mathbb{1} - P_N \mathcal{J} T_{\theta, N}) y_N = P_N f,$$

where \mathfrak{J} denotes the spectral integration (either Fredholm, or Volterra), and $T_{\theta,N}$ indicates a neural network parameterized by θ and that is defined over the space X_N . We consider now also the related problem of “projecting” the IE over X_N by means of the projection $P_N : X \rightarrow X_N$, for a choice of $N > 0$

$$(12) \quad (\mathbb{1} - P_N T)y_N = P_N f$$

in the space X_N . See also Chapter 12 in [5] for a similar procedure. The underlying idea of the method is that since the spaces X_N approximate increasingly well the space X , solving Equation (12) for N large enough produces an approximate solution y_N which is close enough to the solution y of Equation (1). Analogously, when using a parameterized operator (as in Equation (2)), we can solve with high accuracy when N is large enough.

Some questions now arise.

Question 3.1. Firstly, it is of interest to understand whether if $u_N \in X_N$ is a solution of Equation (12) for each given N , we have $\|y - u_N\| \rightarrow 0$ as $N \rightarrow \infty$, where y is the real solution of the IE before projecting it. We observe that while this is naturally expected (cf. with the intuitive idea above), it is not necessarily true.

Question 3.2. Secondly, another important question regards the possibility of approximating projected operators $P_N T : X_N \rightarrow X_N$ through the integral operators in spectral domain described in Section 2. The importance of this question regards the fact that if T is such that $\|y - u_N\| \rightarrow 0$ as $N \rightarrow \infty$, then we can approximate solutions of Equation (1) by knowing solutions of Equation (12), and approximating $P_N T$ would mean that we can approximate the original problem through a neural network in the spectral space with high accuracy (upon choosing N large enough).

Question 3.3. Thirdly, it remains to be understood whether when the first and second problems have positive answer, it is possible to learn the operators $P_N T$, e.g. through Stochastic Gradient Descent, or adjoint methods as in [31].

We start by considering Question 3.1 where we see that in some well-behaved situations solving the projected equation gives an approximate solution of the original equation. We recall that an operator $T : X \rightarrow X$ is said to be bounded if $\|T(y)\| \leq M\|y\|$ for all $y \in X$ and some M . While boundedness and continuity coincide for linear operators, the two concepts are different when dealing with nonlinear operators, as in our situation.

We assume that the integral equation $T(y) + f = y$ admits a solution u that is isolated and of non-zero index for T (see [19]), where u is a Hölder continuous function, i.e. that it belongs to $C^{k,\beta}$ for some k and β . We assume that T is completely continuous and Frechet differentiable, and that T' is bounded, with bound L . These assumptions are not very restrictive, see for instance [19] for several families of integral operators satisfying them. Also, in what follows, we assume that T maps the Hölder space $C^{k,\beta}$ into itself. This simply means that T takes regular enough functions and does not make them less regular. Here we set D to denote a closed ball around 0 in $C^{k,\beta}$ containing u , and we let R denote the image $T(D) = R$. Lastly, we assume that 1 is not an eigenvalue of $T'(u)$, and therefore $(\mathbb{1} - T'(u))^{-1}$ exists and it is bounded.

Theorem 3.4. *In the hypotheses above, the projected equation*

$$P_N T(y_N) + f = y_N$$

admits at least a solution u_N for all N large enough. Moreover,

$$\|u - u_N\| \rightarrow 0$$

as $N \rightarrow \infty$, with the same rate as $\|P_N u - u\| \rightarrow 0$.

Proof. From the fact that the operator T has an isolated fixed point of non-zero index, we deduce that we can apply the framework of [19] Chapter 3 (see also [20]). This gives us that the projected equations eventually admit solutions u_N , and that the projected solutions converge to u , the fixed point of the operator $T + f$. This facts do not depend on the function f appearing in the equation, as one can easily verify directly. Now, we want to show that the numerical scheme converges to u uniformly, at the same rate as $\|P_N u - u\|$. To do so, we proceed as in [6]. We write the equality

$$(\mathbb{1} - T'(u))(u_N - u) = (P_N - \mathbb{1})T'(u)(u_N - u) + (P_N - \mathbb{1})u + P_N[T(u_N) - T(u) - T'(u)(u_N - u)].$$

We then derive the inequalities

$$\begin{aligned} \|u_N - u\| &\leq \|(\mathbb{1} - T'(u))^{-1}T'(u)(u_N - u)\| + \|(\mathbb{1} - T'(u))^{-1}(P_N - \mathbb{1})u\| \\ &\quad + \|(\mathbb{1} - T'(u))^{-1}P_N[T(u_N) - T(u) - T'(u)(u_N - u)]\| \\ &\leq \|(\mathbb{1} - T'(u))^{-1}\| \cdot \|T'(u)\| \cdot \|u_N - u\| + \|(\mathbb{1} - T'(u))^{-1}\| \cdot \|P_N u - \mathbb{1}u\| \\ &\quad \frac{\|(\mathbb{1} - T'(u))^{-1}P_N(T(u_N) - T(u) - T'(u)(u_N - u))\|}{\|u_N - u\|} \cdot \|u_N - u\|. \end{aligned}$$

The fraction $q_N = \frac{\|(\mathbb{1} - T'(u))^{-1}P_N(T(u_N) - T(u) - T'(u)(u_N - u))\|}{\|u_N - u\|}$ goes to zero, as N goes to ∞ from the results of [19, 20]. Moreover, let r denote the radius of the ball D . From the definition of norm in $C^{k,\beta}$, it follows that for all the functions $y \in D$, the Hölder constant $M_k(y)$ is at most r . So, we can uniformly bound the constants on D . For y in the Banach space $C^{k,\beta}$, Jackson's Theorem gives us that

$$\|y - P_N y\| \leq \frac{M_k(y)}{n^{k+\beta}} \leq \frac{r}{n^{k+\beta}} \rightarrow 0.$$

As a consequence, $\|P_N u - u\| \rightarrow 0$ as $N \rightarrow \infty$. In addition we have $\|(P_N - \mathbb{1})T'(u)\| \rightarrow 0$ over D and we can bound $\|P_N\|$ uniformly over D . We therefore obtain

$$\|u_N - u\| \leq \frac{1}{1 - \|(P_N - \mathbb{1})T'(u)\| - \|P_N\|q_N} \|P_N u - u\|,$$

where $\|(P_N - \mathbb{1})T'(u)\| \rightarrow 0$ and $\|P_N\|q_N \rightarrow 0$, and therefore for N large enough this inequality makes sense. We obtain that $\|u_N - u\|$ goes to zero with at least the same speed as $\|P_N u - u\|$, whose convergence to zero depends on k and β , as shown above. We can also get a similar lower bound following an analogous procedure, showing that the speed with which $\|u_N - u\|$ converges to zero is the same as the speed with which $\|P_N u - u\|$ converges to zero. \square

Remark 3.5. Observe that since $\|P_N\| \rightarrow \infty$ as $N \rightarrow \infty$, the previous result does not give that $\|u - u_N\| \rightarrow 0$ always. In fact, from the Uniform Boundedness Principle, we know that there must be functions for which $\|u - P_N u\|$ does not converge to zero. In such cases, the same procedure above cannot be applied. This is somehow inconvenient, but not unexpected. In fact, the Chebyshev expansion is known to not always converge. However, it converges for functions that are regular enough, which is the most important case in applications, especially in physics and engineering.

Remark 3.6. The result above is local in nature, in the sense that we are considering a ball D around zero, in the space $C^{k,\beta}$. The ball has arbitrary radius, as long that it contains the solution u to the integral equation, which is not a very strong condition. However, this hypothesis is needed in order to have that $\|P_N\|$ is uniformly bounded. If we allow the whole space $C^{k,\beta}$ instead of constraining the result on D , we would still have $\|P_N - \mathbb{1}\| \rightarrow 0$ as above, since this is obtained

through a bound deduced from Jackson's Theorem. However, the product $\|P_N\|q_N$ might not go to zero. In this case, the result above would hold if q_N goes to zero faster than \log goes to ∞ , in the sense that $q_N \log N \rightarrow 0$. This is because $\|P_N\| \rightarrow \infty$ on $C^{k,\beta}$ as $\log N$.

There is a consideration regarding the method of Section 2 in relation to the result of Theorem 3.4. In fact, as in any collocation method, the spectral approach followed in this article produces solutions at the collocation points $\{t_i\}$, while in Theorem 3.4 the functions u_N are assumed to be solutions for all t (i.e. not only at the collocation points). We momentarily leave aside the further issue that we only obtain approximate solutions at the collocation points. As a consequence, we can consider that for each N we obtain an interpolation of the function u_N . However, we observe that it is known that for a function ξ which is $N + 1$ times continuously differentiable, the error for a Chebyshev interpolation Π_N of degree $N + 1$ is bounded as

$$\|\xi - \Pi_N\|_\infty \leq \frac{K_N}{2^N(N+1)!},$$

where $K_N = \max_{[-1,1]} |\xi^{N+1}|$, and the points t_i of interpolation are assumed to be the Chebyshev nodes. As a consequence, we can obtain solutions u_N with arbitrarily high precision through the described collocation method. We point out that, in general, a dataset might require points t_i that do not coincide with the Chebyshev nodes, in which case the polynomial interpolation would not be "optimal". We show that our algorithm still works in such situations with good accuracy by means of experimentation. See Section 5, where the data points are not assumed to be at the Chebyshev nodes.

We now turn to Question 3.2. We assume here that the operator $T : X \rightarrow X$ is defined through a kernel G that is continuous in all three variables y, t and s , and it is therefore a continuous operator with respect to the uniform norm. Here X is a space of continuous functions depending on the problem (e.g. continuous functions with some fixed boundary in $[-1, 1]$).

Lemma 3.7. *With notation and assumptions as above, let T denote a Fredholm or Volterra integral operator, and let $P_N T : X_N \rightarrow X_N$ be its projection on X_N . Then, for any fixed $\epsilon > 0$, there exist neural networks $F_N, g_N : X_N \rightarrow X_N$ that satisfy the condition*

$$\|P_N T(y) - P_N \mathfrak{J} F_N(y) - g_N(y)\|_\infty < \epsilon,$$

for all $y \in X_N$, where \mathfrak{J} denotes the spectral integration in Fredholm or Volterra form (depending on T). Moreover, $P_N \mathfrak{J} F_N$ approximates with arbitrarily high precision the operator defined through: $P_N \int_{-1}^{\alpha(t)} P_N G(y, t, s) ds$.

Proof. We focus on the case of Fredholm operators, but the reasoning given here can be applied also to the case of Volterra operators with minor modifications.

Since $y \in X_N$, it follows that any such function can be expressed as a linear combination $y(s) = \sum_{i=0}^N a_i C_i(s)$. Therefore, the operator $T(y)$ induces a function $\mathfrak{T} : \mathbb{R}^{N+1} \times [-1, 1] \rightarrow \mathbb{R}$ through the assignment

$$(a_0, \dots, a_N, t) \mapsto T\left(\sum_i a_i C_i\right)(t).$$

Since T is continuous with respect to the uniform norms, we can show that \mathfrak{T} is continuous as well, where the domain is endowed with the standard Euclidean norm. In fact, for a tuple $(a_{0,1}, \dots, a_{N,1}, t_1) \in \mathbb{R}^{N+1} \times [-1, 1]$, and an arbitrary choice of $\epsilon > 0$, from the uniform continuity of T we can find δ' such that $\max_s |y_1(s) - y_2(s)| < \delta'$ implies that $\max_t |T(y_1)(t) - T(y_2)(t)| < \epsilon/2$, where $y_k := \sum_i a_{i,k} C_i$, for $k = 1, 2$. Then, taking a ball $B = \mathbb{B}_{\frac{\delta'}{N+1}}(a_{0,1}, \dots, a_{N,1}, t_1)$ of radius $\frac{\delta'}{N+1}$

centered in $(a_{0,1}, \dots, a_{N,1}, t_1)$ we have that $|y_1(s) - y_2(s)| = |\sum_i (a_{i,1} - a_{i,2}) C_i(s)| \leq \sum_i |a_{i,1} - a_{i,2}| < \delta'$, whenever $(a_{0,2}, \dots, a_{N,2}, t_2)$ is taken in B . This in turn implies that $|T(y_1)(t) - T(y_2)(t)| < \epsilon/2$ for all $t \in [-1, 1]$. Since $T(y_1)$ is a continuous function with respect to t , we can find δ'' such that $|T(y_1)(t_1) - T(y_1)(t_2)| < \epsilon/2$ whenever $|t_1 - t_2| < \epsilon/2$. Choosing $\delta = \min\{\frac{\delta'}{N+1}, \delta''\}$, we have

$$\begin{aligned} |T(y_1)(t_1) - T(y_2)(t_2)| &= |T(y_1)(t_1) - T(y_1)(t_2) + T(y_1)(t_2) - T(y_2)(t_2)| \\ &\leq |T(y_1)(t_1) - T(y_1)(t_2)| + |T(y_1)(t_2) - T(y_2)(t_2)| \\ &< \epsilon/2 + \epsilon/2 = \epsilon, \end{aligned}$$

whenever $(a_{0,2}, \dots, a_{N,2}, t_2) \in \mathbb{B}_\delta(a_{0,1}, \dots, a_{N,1}, t_1)$. Using the definition of \mathfrak{T} , this implies that \mathfrak{T} is continuous as claimed.

Now, using the spectral integration (Section 2), we can write $T(y)(t)$ by first decomposing $G(y, t, s)$ in a Chebyshev series $\sum_i b_i(t) C_i$ for any t , and then integrating it through the mapping \mathfrak{J} . Since G depends both on $y \in X_N$ and t , the coefficients b_i are functions of the coefficients a_i that uniquely determine y , and the variable t , i.e. they are of the form $b_i(a_0, \dots, a_N, t)$. We want to show now that they are continuous functions $\mathbb{R}^{N+1} \times [-1, 1] \rightarrow \mathbb{R}$. To do so, first recall that the Chebyshev coefficients of $G(y, t, s)$ (for fixed t) are found through the formula

$$b_k = \frac{2}{\pi} \int_{-1}^1 \frac{G(y, t, s) C_k(s)}{\sqrt{1-s^2}} ds.$$

As seen above, for all $s \in [-1, 1]$ we have $|y_1(s) - y_2(s)| \leq \sum_i |a_{i,1} - a_{i,2}|$ for functions in X_N , from which we have that using the continuity of G , for any choice of $\epsilon > 0$, we can find $\delta > 0$ small enough such that $|G(y_1(s), t_1, s) - G(y_2(s), t_2, s)| < \epsilon/2$ whenever $(a_{0,2}, \dots, a_{N,2}, t_2) \in \mathbb{B}_\delta(a_{0,1}, \dots, a_{N,1}, t_1)$. Now, we have

$$\begin{aligned} &|b_k(a_{0,1}, \dots, a_{N,1}, t_1) - b_k(a_{0,2}, \dots, a_{N,2}, t_2)| \\ &= \frac{2}{\pi} \left| \int_{-1}^1 \{G(y_1(s), t_1, s) - G(y_2(s), t_2, s)\} \frac{C_k(s)}{\sqrt{1-s^2}} ds \right| \\ &\leq \frac{2}{\pi} \int_{-1}^1 |G(y_1(s), t_1, s) - G(y_2(s), t_2, s)| \frac{|C_k(s)|}{\sqrt{1-s^2}} ds \\ &< \frac{2}{\pi} \frac{\epsilon}{2} \int_{-1}^1 \frac{1}{\sqrt{1-s^2}} ds = \epsilon, \end{aligned}$$

whenever $(a_{0,2}, \dots, a_{N,2}, t_2) \in \mathbb{B}_\delta(a_{0,1}, \dots, a_{N,1}, t_1)$, showing the continuity of $b_k : \mathbb{R}^{N+1} \times [-1, 1] \rightarrow \mathbb{R}$ for any arbitrary k .

Now, from the continuity of the coefficients b_k , it follows that we can find neural networks f_k of some depth and width ([25]) such that $|b_k - f_k| < \frac{\epsilon}{2(N+1)}$ on $\mathbb{R}^{N+1} \times [-1, 1]$, for $k = 0, \dots, N+1$. Since the spectral integration creates a linear combination of the coefficients b_k , we have that setting $F_N = \sum_i f_i$ the inequality $|\mathfrak{J}P_N G - \mathfrak{J}F_N| < \epsilon/2$ holds on all $\mathbb{R}^{N+1} \times [-1, 1]$, i.e. for all $y \in X_N$. Since the b_k are continuous and $T(y)(t)$ is continuous as well (with respect to a_i and t), we can find a neural network $g_N : \mathbb{R}^{N+1} \times [-1, 1] \rightarrow \mathbb{R}$ which satisfies $|T(y)(t) - \mathfrak{J}P_N G - g_N| < \epsilon/2$ on $\mathbb{R}^{N+1} \times [-1, 1]$ (again [25]). This means that on $\mathbb{R}^{N+1} \times [-1, 1]$ we have $\|P_N T(y) - P_N \mathfrak{J}F_N(y) - g_N(y)\|_\infty < \epsilon$, and moreover F_N approximates the projected integral operator over X_N with arbitrary precision. To complete, now we apply the projector P_N and since this is continuous, the approximation properties found above are preserved (possibly upon choosing an ϵ' appropriately in the previous discussion). \square

Remark 3.8. We can use other universal approximation results such as [17], instead of [25], to derive the approximation capabilities of spectral integral neural networks. Depending on the results used, some extra assumptions need to be imposed on F_N and g_N , but the gain is that simpler architectures might be used. For instance, in [17], one finds that a single layer neural network can locally (i.e. in some closed ball) approximate integral operators.

Theorem 3.9. *Let $T(y) + f = y$ be an integral equation where T satisfies the hypotheses of Theorem 3.4, and that admits a unique solution $u \in C^{k,\beta}$. Then, for any $\epsilon > 0$ we can find $N > 0$, and neural networks G , g and \tilde{f} such that if \tilde{u} is the solution of $P_N \mathfrak{J}G(y) + g(y) + \tilde{f} = y$ which we assume to have solutions for N large enough for any \tilde{f} , we have $\|u - \tilde{u}\|_\infty < \epsilon$.*

Proof. For N large enough, $P_N \mathfrak{J}G(y) + g(y) + \tilde{f} = y$ has a solution \tilde{u}_N and we can write

$$\|u - \tilde{u}_N\| \leq \|u - u_N\| + \|u_N - \tilde{u}_N\|,$$

where u_N is the solution to the projected equation $P_N T(y) + P_N f = y$ as in the case of Theorem 3.4. Then, we can choose N large enough such that $\|u - u_N\| < \epsilon/2$, since $\|u - u_N\| \rightarrow 0$. From Lemma 3.7 we can find neural networks G and g such that

$$\|P_N T(y) - P_N \mathfrak{J}G(y) - g(y)\| < \epsilon/4,$$

for all y in X_N , the projection space of continuous functions (in particular the projection of the Hölder space). Since f is continuous, we can also choose (via the Universal Approximation Theorem) a neural network \tilde{f} such that

$$\|P_N f - \tilde{f}\| < \epsilon/4.$$

Then, from the definition of u_N and \tilde{u}_N we have

$$\|u_N - \tilde{u}_N\| = \|P_N T(u_N) + P_N f - P_N \mathfrak{J}G(y) - g(y) - \tilde{f}\| \leq \epsilon/4 + \epsilon/4.$$

Therefore, we find that for N large enough, $\|u - \tilde{u}_N\| < \epsilon$, which completes the proof. \square

We can also derive the following result, which shows that we can at least locally approximate continuous bounded operators in Hölder spaces through the methods considered in this article.

Theorem 3.10. *Let T be an integral operator (Fredholm or Volterra) defined on the Hölder space $C^{k,\beta}$. Then, for any choice of $\epsilon > 0$, we can find $N > 0$ and neural networks G and g for which*

$$\|T(y) - P_N \mathfrak{J}G(y) - g(y)\|_\infty < \epsilon,$$

for all $y \in \mathbb{B}(0, r)$, where $\mathbb{B}(0, r)$ is an arbitrary radius- r ball centered at zero in $C^{k,\beta}$.

Proof. For any y and any choice of neural networks G and g we use the projection P_N to obtain

$$\begin{aligned} \|T(y) - P_N \mathfrak{J}G(y) - g(y)\|_\infty &= \|T(y) - P_N T(y) + P_N T(y) - P_N \mathfrak{J}G(y) - g(y)\|_\infty \\ &\leq \|T(y) - P_N T(y)\|_\infty + \|P_N T(y) - P_N \mathfrak{J}G(y) - g(y)\|_\infty \\ &\leq \frac{M_k(y)}{N^{k+\beta}} + \|P_N T(y) - P_N \mathfrak{J}G(y) - g(y)\|_\infty. \end{aligned}$$

Let us now choose an arbitrary r and select N such that $\frac{r}{N^{k+\beta}} < \epsilon/2$. Now, from Lemma 3.7 we can find G and g such that $\|P_N T(y) - P_N \mathfrak{J}G(y) - g(y)\|_\infty < \epsilon/2$, which completes the proof. \square

Remark 3.11. A generalization of the previous result to Sobolev spaces, using the results of [9], would be of theoretical interest.

Remark 3.12. Lastly, we observe that in several cases in practice, one is interested in studying the equation

$$\lambda T(y) + f = y,$$

where λ is a nonzero parameter which is useful to determine, when λ is small enough, the existence and uniqueness of the solutions of the integral equation, e.g. through fixed point iterations. See [19], Chapter 3, for examples. This is substantially equivalent to an eigenvalue problem for nonlinear operators (for nonzero eigenvalues), where the definition of eigenvalue of T is defined in the “naive” way as in [19]. See [7] for an overview of spectral theory for nonlinear operators.

Regarding Question 3.3, an approach similar to the one pursued in [31] can be applied here to show that the gradient descent method can be applied to the architecture proposed in this article to obtain the neural networks G and g . However, we do not adapt those methods to our case, but rather content ourselves with showing that gradient descent is possible by means of experimentation.

4. ALGORITHM

The considerations up to now do not take into account the fact that the approximated (projected) equation needs to be solved using some numerical scheme. Therefore, the theoretical bounds obtained in Section 3 assume an exact solution of the projected equation. This is obviously not the case in practice, and we should introduce some numerical solver scheme to obtain the solutions u_N .

Our algorithm, therefore, is based on projecting the equation as described in Section 3, and then solving the corresponding equation. Gradient descent is performed on the error between the solution obtained, and the target function. The function f is used for initialization of the solver, and it is obtained from the available data. For instance, if the problem is to predict a dynamics from the initial 5 time points, these 5 points are used to obtain the function f , and solving the projected integral equation gives the predicted (approximated) dynamics.

We use the Chebyshev coefficients as inputs of our neural networks, and perform integration on the output function (identified with its coefficients) through the spectral integration \mathfrak{J} described in Section 2. To solve the projected equation, we use a fixed point iteration in the projected coefficient space. While the fixed point iteration is guaranteed to converge under the more restrictive assumptions of contractivity of the operator, we see that in practice such convergence is achieved in our experiments. In more delicate cases, one might introduce extra constraints to guarantee the convergence of the iterations.

The method is schematically described in Algorithm 1.

5. EXPERIMENTS

We showcase the algorithm described in Section 4 on two classes of experiments. We consider a dataset consisting of solutions of an integral equation solved numerically. The kernel of the integral operator consists of matrices with hyperbolic functions entries in the variables t and s , where the latter is the variable of integration. The second dataset is a simulated fMRI dataset generated by solving a delayed ODE system that describes the behavior of neurons in the brain.

We show that the model can predict the dynamics, and show that the memory footprint of the model is very low, considering that it is solving an integral equation for each epoch. Moreover, we perform interpolation experiments to demonstrate that the model is very stable with respect to variations in the temporal domain of train and evaluation. We have chosen datasets with nonlocal

Algorithm 1 Algorithm for the spectral neural integral equation model.

Require: Integrand neural network G_θ and f \triangleright Initial model and function f obtained from the available data

Ensure: Trained neural network G_θ \triangleright Solution of Equation (5) projected in N -dimensional space

1: Project dataset on N -dimensional space X_N using $P_N = \sum_{k=0}^{N-1} \frac{2}{\pi} \int_{-1}^1 \frac{F(s)C_k(s)}{\sqrt{1-s^2}} ds \cdot C_k$

2: Initialize iterations with function $u_0 := f$

3: **while** While $\|u_k - u_{k+1}\| > \tau$ **do** \triangleright Solve Equation (5) iteratively in X_N

4: $u_{k+1} = \mathcal{J}G_\theta(u_k) + f$

5: **end while**

6: Solution u_N \triangleright Output of the iterative procedure

7: Convert u_N to an approximate solution in original space, y_N \triangleright Use Chebyshev interpolation

8: Compute $\|y_N - u\|$ \triangleright Evaluate the error between y_N and data u

9: Use gradients computed while solving Equation (5) to perform gradient descent to optimize G_θ

behaviors, like integral equations and delay differential equations, to explore the capability of the model to model long range temporal dependencies in the datasets.

5.1. Integral Equations Dataset. In this experiment, the model is initialized using two points for each dynamics. The task is to predict the whole dynamics, which consists of 100 time points. To test the capability of the model to interpolate, we train our Spectral NIE on a downsampled dataset that contains half of the points of the curves. During evaluation, the model then outputs 100 points, even though it has been trained on 50 time points alone. Convergence of the model is considered to be 200 epochs with no improvement on the validation set. The walltime of the experiment is the time elapsed between the beginning of the training to the convergence, as per the aforementioned criterion. An upper bound of one hour training has been fixed, and models that did not converge within this time are reported as having walltime > 3600 .

In Table 1 we have reported two different Spectral NIE models, a large model with more than 100K paramters, and a small model with only 316 parameters. For both models, the MC represents the number of points used to perform the Monte Carlo integration used in the interpolation. We see that increasing MC by a 10-fold factor we obtain a faster convergence time, but higher memory footprint.

For the other models, we have also tested ANIE (which is an implementation of the original NIE of [30]) with two models, a large one and a small one, with number of parameters comparable to the corresponding Spectral NIE models. We find that for small models, the Spectral NIE model has a significantly better performance than ANIE, with smaller walltime and one order of magnitude better interpolation. For the larger models, we observe that Spectral NIE has better memory footprint and better walltime, but ANIE has a slightly better overall performance in terms of error and interpolation error. Moreover, we see that the memory footprint of the Spectral NIE grows slowly with respect to the size of the model, since most of the computational expense is due to the Monte Carlo integration used for interpolation, and therefore independent on the model itself. ANIE’s complexity, however, grows faster with respect to the size of the model.

Among the other models that we have tested for comparison, we also have ResNet, LSTM, Nerual Ordinary Differential Equation (its newer Latent ODE variant), and Fourier Neural Operator (FNO). No surprisingly, both the integral equation based models perform significantly better than

these models, since they either do not implement nonlocal dynamics or, as in the case of LSTM, their nonlocality properties are limited.

In Table 1, Error refers to the mean squared error of the predicted dynamics with respect to the real dynamics when trained over the full time interval (no downsampling). Interpolation error refers to the setup where the dataset is downsampled for training, and the prediction of the model is performed over the full time interval. The experiment shows that the model is quite stable with respect to changes of time interval between train and evaluation. We think that such stability is due to the use of spectral methods, which automatically give a set of polynomials that can be evaluated on arbitrary points, resulting in good interpolation results.

Models	Memory (MiB)	Walltime (sec)	Error (MSE)	Interp Error (MSE)	Parameters
Spectral NIE (MC = 1K)	74	165.21	0.0022 ± 0.0016	0.0028 ± 0.0032	126498
Spectral NIE (MC = 10K)	324	408.04	0.0032 ± 0.0022	0.0035 ± 0.0024	316
Spectral NIE (MC = 1K)	68	546.50	0.0025 ± 0.0013	0.0026 ± 0.0014	316
ANIE (Large)	122	564.94	0.0014 ± 0.0002	0.0015 ± 0.0003	135363
ANIE (Small)	44	1111.74	0.0062 ± 0.0009	0.01175 ± 0.0017	531
ResNet	42	305.47	0.4269 ± 0.0588	0.2619 ± 0.0343	30802
LatentODE	40	> 3600	0.6342 ± 0.2838	0.6290 ± 0.2813	1428
LSTM (init 10)	102	262.90	0.1785 ± 0.0942	NA	41802
LSTM (init 20)	122	864.66	0.0492 ± 0.0110	0.1707 ± 0.1285	41802
FNO1D (init 5)	258	> 3600	0.0292 ± 0.0285	0.0994 ± 0.1207	287843
FNO1D (init 10)	250	3488.40	0.0286 ± 0.0268	0.1541 ± 0.2724	288163

TABLE 1. Experimental results for the Integral Equations Dataset. Both errors are reported as mean squared errors.

5.2. Simulated fMRI Dataset. We consider now a simulated fMRI dataset. This is generated using the package `neurolib` [8] through a system of delay differential equations that simulate the stimulus of brain regions. The dynamics is 80 dimensional, and each dimension refers to a brain region. Moreover, the system has a high degree of nonlocality.

We consider different types of initializations, where we assume that 3, 4 or 7 time points are available for initialization of the model. Clearly, as the number of available points for initialization increases, the models' predictions become more accurate, since the task is simpler.

N init	Spectral NIE	ANIE	NODE	LSTM	FNO1D
3	0.0027 ± 0.0006	0.0090 ± 0.0092	0.1189 ± 0.0437	0.0871 ± 0.0146	0.0794 ± 0.0150
4	0.0025 ± 0.0007	0.0096 ± 0.0097	0.1102 ± 0.0243	0.0819 ± 0.0145	0.0726 ± 0.0130
7	0.0012 ± 0.0006	0.0069 ± 0.0113	0.1138 ± 0.0302	0.0810 ± 0.0136	0.0576 ± 0.0100

TABLE 2. Experimental results for fMRI simulated dataset: all reported values refer to mean squared error. The models are initialized with varying amount of time points.

Table 2 shows the results of the experiment, where we have compared the Spectral NIE to ANIE, NODE, LSTM and FNO1D. In all experiments, the number of parameters of the model are comparable, to ensure a more meaningful comparison. Once again, since the dynamics is highly

nonlocal, we expect that integral equation based models perform better. This is indeed the case, as shown in the table. Moreover, we see that Spectral NIE performs significantly better than ANIE in this experiment, and the gain in using our spectral approach is not only in computational cost and convergence time, but also in accuracy.

Example predictions for the Spectral NIE for 3, 4 and 7 initialization points are given in Figure 1, Figure 2 and Figure 3, respectively. In all figures, the top dynamics represents the prediction, and the bottom dynamics represents the ground truth. The \vec{x} -axis represents all the 80 brain locations, while the \vec{y} -axis refers to the 20 time points per dynamics.

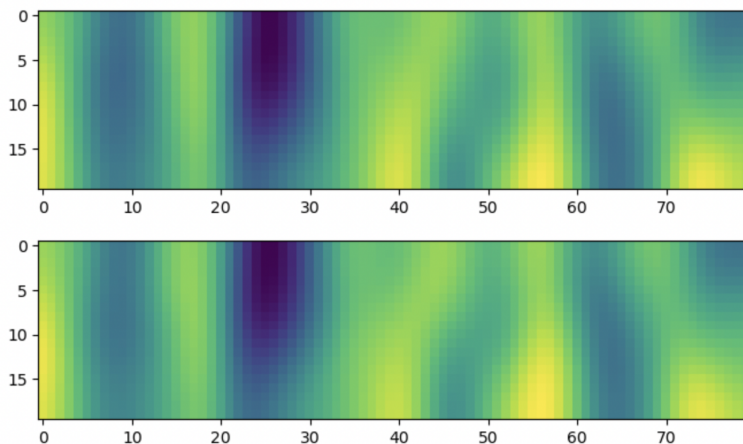


FIGURE 1. Example prediction for Spectral NIE on fMRI Dataset with 3 time points used for initialization. Top: Prediction. Bottom: Ground truth.

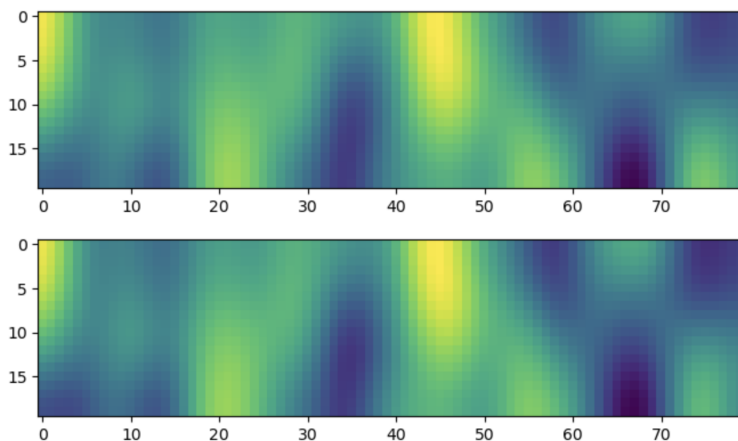


FIGURE 2. Example prediction for Spectral NIE on fMRI Dataset with 4 time points used for initialization. Top: Prediction. Bottom: Ground truth.

REFERENCES

- [1] FT Adler, *Reactor kinetics: integral equation formulation*, Journal of Nuclear Energy. Parts A/B. Reactor Science and Technology **15** (1961), no. 2-3, 81–85.
- [2] Shun-ichi Amari, *Dynamics of pattern formation in lateral-inhibition type neural fields*, Biological cybernetics **27** (1977), no. 2, 77–87.

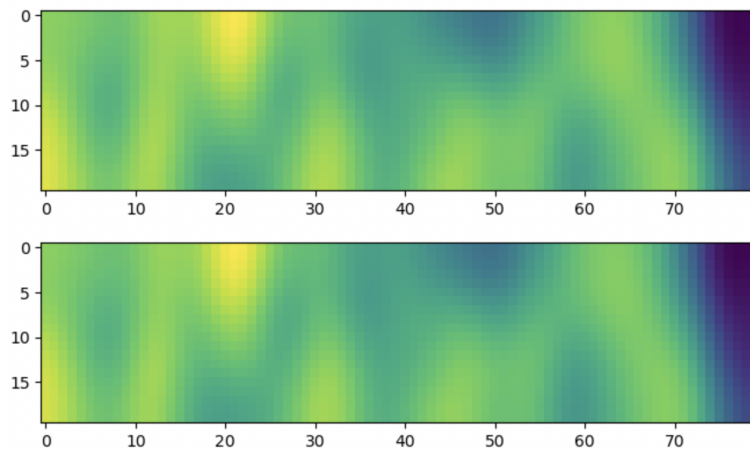


FIGURE 3. Example prediction for Spectral NIE on fMRI Dataset with 7 time points used for initialization. Top: Prediction. Bottom: Ground truth.

- [3] John D Anderson, *Governing equations of fluid dynamics*, Computational fluid dynamics: an introduction (1992), 15–51.
- [4] Kendall E Atkinson, *A survey of numerical methods for the solution of Fredholm integral equations of the second kind*, Society of Industrial and Applied Mathematics (1976).
- [5] Kendall Atkinson and Weimin Han, *Theoretical numerical analysis*, Vol. 39, Springer, 2005.
- [6] Kendall E Atkinson and Florian A Potra, *Projection and iterated projection methods for nonlinear integral equations*, SIAM journal on numerical analysis **24** (1987), no. 6, 1352–1373.
- [7] Alessandro Calamai, Massimo Furi, and Alfonso Vignoli, *An overview on spectral theory for nonlinear operators*, Communications in Applied Analysis **13** (2009), no. 4, 509–534.
- [8] Caglar Cakan, Nikola Jajcay, and Klaus Obermayer, *neurolib: a simulation framework for whole-brain neural mass modeling*, Cognitive Computation (2021), 1–21.
- [9] Claudio Canuto and Alfio Quarteroni, *Approximation results for orthogonal polynomials in Sobolev spaces*, Mathematics of Computation **38** (1982), no. 157, 67–86.
- [10] Salvatore Capozziello and Francesco Bajardi, *Nonlocal gravity cosmology: An overview*, International Journal of Modern Physics D **31** (2022), no. 06, 2230009.
- [11] Leonard Michael Delves and Julie L Mohamed, *Computational methods for integral equations*, CUP Archive, 1988.
- [12] Odo Diekmann, *On a nonlinear integral equation arising in mathematical epidemiology*, North-Holland Mathematics Studies, 1978, pp. 133–140.
- [13] David Gottlieb and Steven A Orszag, *Numerical analysis of spectral methods: theory and applications*, SIAM, 1977.
- [14] Leslie Greengard, *Spectral integration and two-point boundary value problems*, SIAM Journal on Numerical Analysis **28** (1991), no. 4, 1071–1080.
- [15] Gaurav Gupta, Xiongye Xiao, and Paul Bogdan, *Multiwavelet-based operator learning for differential equations*, Advances in neural information processing systems **34** (2021), 24048–24062.
- [16] Zhongkai Hao, Zhengyi Wang, Hang Su, Chengyang Ying, Yinpeng Dong, Songming Liu, Ze Cheng, Jian Song, and Jun Zhu, *Gnot: A general neural operator transformer for operator learning*, International Conference on Machine Learning, 2023, pp. 12556–12569.
- [17] Kurt Hornik, Maxwell Stinchcombe, and Halbert White, *Multilayer feedforward networks are universal approximators*, Neural networks **2** (1989), no. 5, 359–366.
- [18] Nikola B Kovachki, Zongyi Li, Burigede Liu, Kamyar Azizzadenesheli, Kaushik Bhattacharya, Andrew M Stuart, and Anima Anandkumar, *Neural Operator: Learning Maps Between Function Spaces With Applications to PDEs.*, J. Mach. Learn. Res. **24** (2023), no. 89, 1–97.
- [19] Yu P Krasnosel’skii, *Topological methods in the theory of nonlinear integral equations*, Pergamon Press (1964).

- [20] MA Krasnosel'skii and PP Zabreiko, *Geometrical Methods of Nonlinear Analysis*, Springer-Verlag, Berlin, 1984, MR 85b **47057**.
- [21] Vangipuram Lakshmikantham, *Theory of integro-differential equations*, Vol. 1, CRC press, 1995.
- [22] Chensen Lin, Zhen Li, Lu Lu, Shengze Cai, Martin Maxey, and George Em Karniadakis, *Operator learning for predicting multiscale bubble growth dynamics*, The Journal of Chemical Physics **154** (2021), no. 10.
- [23] Yucheng Liu, *Application of the Chebyshev polynomial in solving Fredholm integral equations*, Mathematical and Computer Modelling **50** (2009), no. 3-4, 465–469.
- [24] Lu Lu, Pengzhan Jin, Guofei Pang, Zhongqiang Zhang, and George Em Karniadakis, *Learning nonlinear operators via DeepONet based on the universal approximation theorem of operators*, Nature Machine Intelligence **3** (2021), no. 3, 218–229.
- [25] Zhou Lu, Hongming Pu, Feicheng Wang, Zhiqiang Hu, and Liwei Wang, *The expressive power of neural networks: A view from the width*, Advances in neural information processing systems **30** (2017).
- [26] Peter Schiavone, Christian Constanda, and Andrew Mioduchowski, *Integral methods in science and engineering*, Springer Science & Business Media, 2002.
- [27] Z Sedláček, *Electrostatic oscillations in cold inhomogeneous plasma Part 2. Integral equation approach*, Journal of Plasma Physics **6** (1971), no. 1, 187–199.
- [28] Hugh R Wilson and Jack D Cowan, *Excitatory and inhibitory interactions in localized populations of model neurons*, Biophysical journal **12** (1972), no. 1, 1–24.
- [29] Changqing Yang, *Chebyshev polynomial solution of nonlinear integral equations*, Journal of the Franklin Institute **349** (2012), no. 3, 947–956.
- [30] Emanuele Zappala, Antonio Henrique de Oliveira Fonseca, Josue Ortega Caro, and David van Dijk, *Neural Integral Equations*, arXiv:2209.15190 (2022).
- [31] Emanuele Zappala, Antonio H de O Fonseca, Andrew H Moberly, Michael J Higley, Chadi Abdallah, Jessica A Cardin, and David van Dijk, *Neural integro-differential equations*, Proceedings of the AAAI Conference on Artificial Intelligence, 2023, pp. 11104–11112.

DEPARTMENT OF MATHEMATICS AND STATISTICS, IDAHO STATE UNIVERSITY, PHYSICAL SCIENCE COMPLEX —
921 S. 8TH AVE., STOP 8085 — POCA TELLO, ID 83209

Email address: emanuelezappala@isu.edu